To be submitted to British Journal of Pharmacology (BJP)

2016-BJP-0946-RP – REVISION

Human podocytes express functional thermosensitive transient receptor potential vanilloid (TRPV) channels

Running title: TRPV channels in human podocytes

Lídia Ambrus[1], Balázs Kelemen[1], Tamás Szabó[2], Tamás Bíró[1,3*], Balázs István Tóth[1*]

[1]DE-MTA "Lendület" Cellular Physiology Research Group, Department of Physiology, Medical Faculty, University of Debrecen, Hungary

[2]Department of Pediatrics, Medical Faculty, University of Debrecen, Hungary

[3]Department of Immunology, Medical Faculty, University of Debrecen, Hungary

*TB and BIT contributed equally to the work

Correspondence to:
Tamás Bíró, MD, PhD, DSc
Department of Immunology, Faculty of General Medicine
University of Debrecen
H-4032 Debrecen, Egyetem tér 1.
Office Phone: +36 52 411-717/65242
FAX: +36 52 417-159
Email: biro.tamas@med.unideb.hu

Number of figures: 5

This article has been accepted for publication and undergone full peer review but has not been through the copyediting, typesetting, pagination and proofreading process which may lead to differences between this version and the Version of Record. Please cite this article as doi: 10.1111/bph.14052

Abstract

BACKGROUND AND PURPOSE

Heat sensitive transient receptor potential vanilloid (TRPV) channels are expressed in various epithelial tissues regulating, among else, barrier functions. Their expression is well established in the distal nephron; however, we have no data about their presence in podocytes. Since podocytes are indispensable in the formation of the glomerular filtration barrier, we investigated the presence and function of Ca^{2+}-permeable TRPV1-4 channels in human podocyte cultures.

EXPERIMENTAL APPROACH

The expression of TRPV1-4 was investigated at protein (immunocytochemistry, western blot) and mRNA (Q-PCR) level in a conditionally immortalized human podocyte cell line. The channel functionality was assessed by measuring intracellular Ca^{2+} concentration using fluo-4 Ca^{2+}-indicator dye and patch clamp electrophysiology upon applying various activators and inhibitors.

KEY RESULTS

Thermosensitive TRP channels were expressed in podocytes. The TRPV1 specific agonists capsaicin and resiniferatoxin did not induce any alteration in the intracellular Ca^{2+} concentration. Cannabidiol, an activator of TRPV2 and TRPV4 induced moderate Ca^{2+}-influxes which were inhibited by both tranilast and HC067047, blockers of TRPV2 and TRPV4, respectively. The TRPV4-specific agonists GSK1016790A and 4α-Phorbol 12,13-didecanoate resulted robust Ca^{2+}-signals which were abolished in the presence of HC067047. Non-specific agonists of TRPV3 induced marked Ca^{2+} transients. However, TRPV3 blockers, ruthenium red and isopentenyl diphosphate only partially inhibited the responses and TRPV3 silencing was ineffective suggesting remarkable off-target effects of the compounds.

CONCLUSION AND IMPLICATIONS

Our results indicate the functional presence of TRPV4 and other thermosensitive TRPV channels in human podocytes and raise the possibility of their involvement in the regulation of glomerular filtration barrier.

Abbreviations

2-APB, 2-Aminoethoxydiphenyl borate

4-αPDD, 4α-Phorbol 12,13-didecanoate

ACTB, β-actin

CBD, cannabidiol

DAPI, 4',6-diamidino-2-phenylindole

FSGS, focal segmental glomerulosclerosis

GAPDH, glyceraldehyde-3-phosphate dehydrogenase

IP3, inositol trisphosphate

IPP, Isopentenyl diphosphate

PPIA, peptidylprolyl isomerase A

Q-PCR, Quantitative Real-Time PCR

RTX, resiniferatoxin

TRP, transient receptor potential

TRPC, transient receptor potential canonical

TRPM, transient receptor potential melastatin

TRPP, transient receptor potential polycystin

TRPV, transient receptor potential vanilloid

Introduction

Among voltage gated ion channels, transient receptor potential (TRP) ion channels form a heterogeneous group with diverse functions. They are sensitive for various physical stimuli, like osmotic challenges, mechanical stimulation, changes of membrane potential or environmental temperature. Therefore, they are generally considered as multimodal cellular sensors. Moreover, TRP channels possess marked chemosensitivity, as well. They can be activated or inhibited by several endogenous or exogenous chemical ligands opening a huge field for potential pharmacological interventions (Nilius and Szallasi, 2014). Amongst TRP channels, the thermosensitive members are the most pursued drug targets especially because of their vital role in several sensory functions (Moran et al., 2011). However, thermoTRPs, especially the heat sensitive members of the vanilloid (TRPV) subfamily play an emerging role in epithelial biology and barrier functions, as well (Moran et al., 2011; Nilius and Szallasi, 2014). They are widely expressed in the outer and inner linings of the human body, like in the skin (Tóth et al., 2014), airway epithelia (Grace et al., 2014), endothelium (Earley and Brayden, 2015) or reabsorbing epithelium of kidney tubules (Kassmann et al., 2013).

The expression of several TRP channels is known along the nephron playing important (patho)physiological role in kidney functions (Woudenberg-Vrenken et al., 2009). TRPV5/6 and TRPM6 expressed in the apical membrane of distal tubule epithelium play an essential role in ion homeostasis via ensuring physiological reabsorption of Ca^{2+} and Mg^{2+}, respectively (Dimke et al., 2011). Mutations in TRPP1/2 complex serve as etiological factors in the development of polycystic kidney disease (Retailleau and Duprat, 2014; Tóth and Nilius, 2015). TRPC6 regulates podocytes' function influencing the integrity of the glomerular filtration barrier and playing etiological role in different proteinuric diseases, among else familial focal segmental glomerulosclerosis (FSGS) (Dryer and Reiser, 2010; Tóth and Nilius, 2015).

Regarding the heat sensitive TRPV channels, TRPV4 is expressed in various segments of the urogenital tract, involving distal tubules of the kidney, and it was found playing an important role in cell junction and barrier formation (Janssen et al., 2016). The presence of TRPV1 was also shown in the tubules of the renal cortex and medulla as well as in the wall of the renal pelvis (Feng et al., 2008; Kassmann et al., 2013). Moreover, both TRPV1 and TRPV4 can influence endothelial barrier functions (Alvarez et al., 2006; Yang et al., 2010) which can affect the vascular side of the glomerular filtration barrier. However, we do not bare any data about the expression of these channels in the other component of the glomerular filtration barrier, i.e. podocytes of the Bowman's capsule. Therefore, in the current study, we aimed at

investigating the molecular expression and functionality of heat sensitive TRPV1-4 channels in human podocytes using a conditionally immortalized human podocyte cell culture system.

Methods

Cell culturing

Human podocyte cell line provided by Prof. Hermann Pavenstädt (University Hospital of Münster, Münster, Germany) was established and cultured as described previously (Saleem et al., 2002; Ambrus et al., 2015). In brief, cells were cultured in "permissive" condition in RPMI medium (PAA Laboratories GmbH, Pasching, Austria) supplemented with 10% fetal bovine serum, (Invitrogen, Paisley, UK), 50 U/ml penicillin, 50 μg/ml streptomycin, 1.25 μg/ml Fungizone (both from PPA Laboratories GmbH) and insulin-transferrin-selenium (1:100; Invitrogen) at 33°C to maintain proliferation. Differentiation was induced by switching to "non-permissive" condition transferring cells to 37°C and kept in culture for 7 days. The process of differentiation was evaluated using Western blotting and immunocytochemistry by determining the expression of the podocyte-specific marker podocin and the differentiation marker synaptopodin as show in our previous work (Ambrus et al., 2015). HEK293T cells were cultured in DMEM medium (PAA Laboratories GmbH) supplemented with 10% fetal bovine serum, (Invitrogen), 50 U/ml penicillin, 50 μg/ml streptomycin, 1.25 μg/ml Fungizone (both from PPA Laboratories GmbH) and non-essential aminoacids (Sigma-Aldrich, St Louis, MO, USA).

Antibodies

The following primary antibodies were employed for immunocytochemistry: mouse anti-human TRPV1, rabbit anti-human TRPV4 (both from Novus Biologicals, Littleton, CO, USA), rabbit anti-human TRPV2, rabbit anti-human TRPV3 (both from Abcam, Cambridge, UK). For Western blotting we used goat anti-human TRPV1 (Santa Cruz, Heidelberg, Germany), rabbit anti-human TRPV3, rabbit anti-human TRPV4 (Alomone Labs, Jerusalem, Israel), rabbit anti-human TRPV2 and rabbit-anti-human β-actin (Sigma-Aldrich).

Immunocytochemistry

Human podocytes were cultured and differentiated on glass coverslips in 6-well plates, were fixed by 4% paraformaldehyde containing phosphate-buffered saline (PBS; 115 mM NaCl, 20

mM Na_2PO_4, pH 7.4; all from Sigma-Aldrich) for 10 min at room temperature, and permeabilized by 0.3% Triton-X-100 (Sigma-Aldrich) in PBS for 10 min. Following 30 min incubation in blocking solution (0.3% Triton-X-100 and 1% BSA containing PBS; both from Sigma-Aldrich) at room temperature, cells were probed with the previously mentioned primary antibodies raised against human TRPV1 (1:50), TRPV4 (1:50), TRPV2 (1:100) and TRPV3 (1:100) overnight at 4°C. Following appropriate washing in PBS, coverslips were incubated with Alexa-488®-conjugated goat-anti-mouse and goat-anti-rabbit secondary antibodies (1:200, Invitrogen) for 1 hour at room temperature. Nuclei were counterstained with 4',6-diamidino-2-phenylindole (DAPI, Vector Laboratories, Peterborough, UK). Negative control cells were stained omitting the primary antibodies. Visualization of the proteins was performed by using Zeiss LSM 510 Meta Confocal Microscope (Zeiss, Oberkochen, Germany).

Western blot

Cells were harvested and homogenized in protease inhibitor cocktail (1:100; Sigma-Aldrich) containing detergent mixture (50 mM TRIS HCl, 150 mM NaCl, 1% Triton X-100, 1% Igepal CA 630, 0.5% sodium deoxicholate; Sigma-Aldrich). Protein concentrations were determined by using BCA reagent (Pierce, Rockford, IL, USA) and set to 0.5 µg/ml. Equal amount of protein samples (5 µg/well) were subjected to SDS-PAGE (10% Mini Protean TGX gels, BioRad, Hercules, CA, USA), and transferred to nitrocellulose membranes, by using Trans-Blot® Turbo™ Nitrocellulose Transfer Packs and Trans Blot Turbo System (both from BioRad). Membranes were probed with the corresponding primary antibodies overnight at 4°C. We applied anti-human TRPV1, TRPV2, TRPV4 (1:100) and TRPV3 (1:200) antibodies, diluted in 5% milk containing PBS. As secondary antibodies, horseradish peroxidase-conjugated rabbit anti-goat and goat anti-rabbit IgGs (1:1000, BioRad) were applied and the immunoreactive bands were visualized by a SuperSignal West Pico Chemiluminescent Substrate-Enhanced Chemiluminescence kit (Pierce) using Gel Logic 1500 Imaging System (Kodak, Tokyo, Japan). To assess equal amount of protein in the different samples, we detected β-actin as control using rabbit anti-human β-actin antibody (1:1000, Sigma-Aldrich).

Transient overexpression of human recombinant TRPV channels

To check the specificity of the antibodies used in western blot experiments, we transiently overexpressed human recombinant TRPV1-4 proteins in HEK293T cells and subjected the cell lysates to western blot. HEK293T cells cultured in 96 mm Petri dishes were transfected at 50-60% confluency using TransIT-293 Transfection Reagent (MirusBio, Madison, WI, USA). 36

μl TransIT-293 reagent and 12 μl DNA construct were gently mixed in 600 μl OptiMEM (LifeTechnologies) medium, incubated for ca. 20 min and added to the cell cultures drop by drop. Following an incubation for additional 48 hrs, cells were harvested and subjected for western blot analysis as described above. As DNA constructs, sequence of human TRPV1 was cloned in the pCAGGSM2-IRES-GFP-R1R2 vector and sequences of human TRPV2, TRPV3 and TRPV4 isoforms were cloned in the pCINeoIRES-GFP vector. The constructs were provided by Prof. Thomas Voets (Laboraory of Ion Channel Research, KU Leuven, Leuven, Belgium).

Gene silencing by RNA interference (RNAi)

Human podocytes were seeded in small Petri dishes or in 96-well black-wall/clear-bottom plates (Greiner Bio-One, Kremsmuenster, Austria) suitable for fluorescent measurements in culture medium. After the podocytes' differentiation, medium was changed to fresh culture medium and cells were transfected with siRNA oligonucleotides targeting human TRPV3 (Stealth RNAi, Invitrogene, ID: HSS136315) using Lipofectamine™ RNAiMAX Transfection Reagent and serum-free Optimem (both from Invitrogen). For controls, siRNA Negative Control Duplexes (scrambled RNA, Invitrogen) were employed. 48 hours after transfection cells in Petri dishes were harvested to quantitatively evaluate the efficacy of siRNA-driven silencing by Q-PCR and flourescent Ca-measurements were performed on cells seeded in microplates.

Quantitative Real-Time PCR (Q-PCR)

To determine the quantitative expressions of various TRPs at the mRNA level, Q-PCR was performed on an ABI Prism 7000 sequence detection system (Applied Biosystems, Foster City, CA, USA) using the 5' nuclease assay. Total RNA was isolated using TRIzol (Invitrogen) and reverse-transcribed into cDNA using High Capacity cDNA Reverse Transcription Kit (Applied Biosystems) and then amplified on a GeneAmp PCR System 2400 DNA Thermal Cycler (Applied Biosystems). PCR amplification was performed by using TaqMan primers and probes (assay ID-s: Hs00218912_m1 for TRPV1, Hs00275032_m1 for TRPV2, Hs00376854_m1 for TRPV3 and Hs00222101_m1 for TRPV4; all from Applied Biosystems). As internal controls, transcripts of peptidylprolyl isomerase A (PPIA; assay ID: Hs99999904_m1), glyceraldehyde-3-phosphate dehydrogenase (GAPDH; assay ID: Hs99999905_m1) and β-actin (ACTB; assay

ID: Hs99999903_m1) were determined (all from Applied Biosystems). During the analysis we used the geometric mean of the PPIA, GAPDH and ACTB as reference value.

Fluorescent Ca^{2+} measurements

Fluorescent measurement of cytoplasmic Ca^{2+} concentration was performed by according to our previously optimized protocol: human podocytes were seeded in 96-well/clear-bottom plates (Greiner Bio-One) at a density of 20,000 cells per well in podocyte medium and cultured at "non-permissive" conditions for 7 days. On the 7th day the cells were washed once with Hank's solution ("normal buffer": 136.8 mM NaCl, 5.4 mM KCl, 0.34 mM Na_2HPO_4, 0.44 mM KH_2PO_4, 0.81 mM $MgSO_4$, 1.26 mM $CaCl_2$, 5.56 mM glucose, 4.17 mM $NaHCO_3$, pH 7.2, all from Sigma-Aldrich) containing 1% bovine serum albumin and 2.5 mM Probenecid (both from Sigma-Aldrich) than loaded with 1 μM Fluo-4 AM (Life Technologies Corporation, Carlsbad, CA, USA) dissolved in Hank's solution (100 μl/well) at 37°C for 30 min. The cells were washed three times with Ca^{2+}-containing (normal buffer) or Ca^{2+}-free (Ca^{2+}-free buffer) Hank's solution (100 μl/well). In the Ca^{2+}-free buffer, equimolar glucose substituted for $CaCl_2$. The plates were then placed into a FlexStation 3 fluorescent microplate reader (Molecular Devices, Sunnyvale, CA, USA) and cytoplasmic Ca^{2+} concentration (reflected by fluorescence; λ_{EX}: 494 nm, λ_{EM}: 516 nm) was monitored during application of compounds in various concentrations. During the measurements, cells in a given well were exposed to only one given concentration of the agents. When applying antagonists, cells were pretreated for 30 min and the measurements were carried out in the continuous presence of fixed concentration of the applied antagonist. Experiments were performed in multiple wells and cells in different wells were cultured, differentiated and treated individually and independently. Data are presented as F_1/F_0, where F_0 is the average fluorescence of the baseline (before compound application) and F_1 is the actual fluorescence. During data analysis, n represents individual, independently measured wells.

To investigate the effect of a heat pulse on intracellular Ca^{2+} concentration, podocytes were seeded and differentiated in 35 mm diameter Petri dishes and loaded with 1 μM Fluo-4 AM (Life Technologies). Then, Petri dishes containing 300 μl ambient temperature normal buffer were placed on the stage of an Olympus IX83 inverted fluorescent microscope (Olympus, Tokyo, Japan) and fluo-4 loaded cells were imaged with constant settings in every 9 s, using the autofocus mode between each capturing. During measurement, 1 ml pre-heated solution was pipetted into the petri dishes. Images were captured using an Xcellence Pro live cell

imaging system (Olympus) and analysed in Fiji app running ImageJ software (Schindelin et al., 2012, 2015).

Patch clamp recording

Podocytes were seeded in small Petri dishes and whole cell patch clamp measurements were made by using an Axopatch 1.D amplifier and Clampex 10.2 software (Molecular Devices) on the next day. To record GSK evoked transmembrane currents, experiments were performed in a bath solution containing 150 mM NaCl, 6 mM CsCl, 5 mM CaCl2, 1 mM MgCl2, 10 mM HEPES and 10 mM glucose buffered to pH 7.4 (NaOH), whereas the pipette solution consisted of 100 mM aspartic acid, 20 mM CsCl, 1 mM MgCl2, 0.08 mM CaCl2, 4 mM Na2ATP, 10 mM EGTA, 10 mM HEPES and pH was set to 7.2 using CsOH resulted in ca. 100 mM CsAsp in the final pipette solution. The holding potential was 0 mV and cells were ramped every 2 s from −120 to +100 mV over the course of 400 ms.

Curve fitting

Logistic dose-response curves were fitted using the equation y = A2 + (A1-A2)/(1 + (x/x0)^p) where the calculated parameters are: A1: initial value (y_{min}), A2: final value (y_{max}), x0: center (EC50) and p is the calculated power. Fittings were carried out and parameters were calculated using Origin 9.0 (OriginLab Corporation, Northampton, MA, USA).

Data and statistical analysis

Since the experiments were carried out on cell cultures using objective methods resulting in quantitative, interval scale numeric data which were analyzed by properly chosen statistical methods, we did not count with any influence of the experimenter expectation on the results. Therefore, no randomization and blinding was performed. If it is not mentioned otherwise, data are presented as mean ± SEM. Normality of data was tested by Shapiro-Wilk test in each group. Comparison of means between multiple groups was done by One-Way ANOVA. If F achieved $P<0.05$, pairwise comparison was done by appropriate post-hoc tests. Homogeneity of variances was tested by Levene's test. If no inhomogeneity was found, ANOVA was followed by either Dunnett or Bonferroni post-hoc tests, as appropriate. In case of inhomogeneous variances, Dunnett's T3 test was performed. To compare means of two groups with data not passing normality, Mann-Whitney U-test was performed. In every case, $p<0.05$ values were regarded as significant differences. All statistical analysis was performed using IBM SPSS

Statistics 23.0 (IBM, Armonk, NY, USA). The data and statistical analysis comply with the recommendations on experimental design and analysis in pharmacology (Curtis et al., 2015).

Materials

Capsaicin, capsazepine, eugenol, carvacrol, thymol, 2-Aminoethoxydiphenyl borate (2-APB), 4α-Phorbol 12,13-didecanoate (4α-PDD) and GSK1016790A were obtained from Sigma-Aldrich. AMG 9810, cannabidiol (CBD) and HC067047 were purchased from Tocris Bioscience (Bristol, UK) and resiniferatoxin (RTX) from Santa Cruz (Santa Cruz, CA, USA). Tranilast was bought from Cayman Chemical Company (Ann Arbor, MI, USA). Isopentenyl diphosphate (IPP) was from Echelon Biosciences (Salt Lake City, UT, USA). Ruthenium red was obtained from Research Biochemicals International (Natick, MA, USA).

Nomenclature of Targets and Ligands

Key protein targets and ligands in this article are hyperlinked to corresponding entries in http://www.guidetopharmacology.org, the common portal for data from the IUPHAR/BPS Guide to PHARMACOLOGY (Southan et al., 2016), and are permanently archived in the Concise Guide to PHARMACOLOGY 2015/16 (Alexander et al., 2015).

Results

First, we investigated the molecular expression of heat sensitive TRPV1-4 channels in cultured, differentiated human podocytes. Immunocytochemical staining revealed a general expression of all the investigated proteins in differentiated human podocytes, although the TRPV1 staining showed a relatively weaker signal compared to TRPV2-4 (Figure 1A). For western blot, we have used selected antibodies of which specificity we have checked by probing human recombinant TRPV1-4 overexpressed in human embryonic kidney derived (HEK293T) cell line (Supplementary figure 1.). The selected antibodies detected all the investigated TRPV isoforms both in differentiated and non-differentiated podocytes, although the molecular weight of the detected bands was not fully identical with the size of the bands detected in the recombinant cell line (Figure 1B). The podocytes specific TRPV1 and TRPV2 bands were detected at a minimal higher molecular weight. The specific antibody detected multiple bands of the recombinant TRPV3 among which only one (ca. 60 kDa) was detected in podocytes. Interestingly, the TRPV4 specific antibody detected a very clear single band corresponding to the predicted molecular weight of the TRPV4 in HEK293T cells overexpressing the recombinant channel. However in podocytes, we could detect very intense

signals, but at definitely lower molecular weight. Nevertheless, each protein was detected both in differentiated and undifferentiated cells, as well. Generally, the intensity of all the TRPV1-4 immunoreactivity was found to be decreased–in differentiated podocytes compared to undifferentiated cells. To further assess the quantitative expression of TRPV channels compared to each other, we studied the expression of specific TRPV transcripts by Q-PCR. We found that the expression of TRPV1 and TRPV4 was relatively high, but TRPV2 and TRPV3 were expressed at relatively low levels (Figure 1C).

Since the molecular expression studies revealed a general expression of heat sensitive TRPV channels, we investigated the functional responses for a thermal challenge applying a heat pulse by adding pre-warmed buffer to differentiated podocyte cultures. Since the studied channels are Ca^{2+}-permeable ones, their activity was investigated by monitoring the intracellular Ca^{2+} concentration using the fluorescent Ca^{2+}-sensitive reporter dye Fluo-4 upon heat stimulation. The majority of the cells reacted for the heat pulse with a transient elevation of the intracellular Ca^{2+} concentration (Figure 1D-F, Supplementary video 1-2) which response was not seen upon applying ambient temperature as a stimulus (Figure 1F and Supplementary video 3). These results clearly indicated the presence of heat sensitive Ca^{2+} channels in differentiated human podocytes. However, the applied heat pulse protocol was not specific enough to identify the individual heat sensitive channels and discriminate between the contributions of the different TRPV isoforms which can bare partially overlapping temperature sensitivity in various conditions. Therefore, to judge the functionality of the individual TRPV isoforms, we used various pharmacological tools to activate these channels and assessed their specificity by applying specific antagonist pretreatments, if specific antagonists were available.

Capsaicin, a specific, potent activator of TRPV1 (Caterina et al., 1997), did not induce any remarkable alteration in the intracellular Ca^{2+} concentration of the podocytes up to 1 mM. The presence of TRPV1 specific antagonists capsazepine or AMG 9810 did not influenced the lack of the capsaicin effect (Figure 2A-B). Similarly, the ultrapotent TRPV1 agonist RTX also failed to evoke any response (Figure 2C). These results suggested, that TRPV1, in spite of the relatively high expression of the mRNA transcripts, does not form a functional channel in the cultured, differentiated human podocytes.

The phytocannabinoid cannabidiol, an agonist of both TRPV2 (Qin et al., 2008) and TRPV4 (De Petrocellis et al., 2012), induced a moderate elevation of intracellular Ca^{2+} concentration when applied at ≥10 µM concentration (EC50=10.56±1.28µM – Figure 3.). This effect was mainly eliminated by omitting the Ca^{2+} from the extracellular solution suggesting that cannabidiol activated Ca^{2+}-permeable ion channels in the plasma membrane. The presence

of 75 μM tranilast (Nie et al., 1997), a potent ion channel inhibitor recently used targeting TRPV2 (Hisanaga et al., 2009; Mihara et al., 2010; Perálvarez-Marín et al., 2013), effectively inhibited the cannabidiol induced Ca^{2+} signals suggesting the presence of functionally active TRPV2 channels. However, cannabidiol was also reported as a weak agonist of TRPV4 (De Petrocellis et al., 2012). Therefore, we investigate the involvement of TRPV4 in the cannabidiol induced Ca^{2+} signals and we repeated the experiments in the presence of HC067047, a potent and selective blocker of TRPV4 (Everaerts et al., 2010). 1 μM HC067047 inhibited the cannabidiol induced Ca^{2+} responses ca. as effectively, as tranilast did (Figure 3.), further confirming our previous results that cannabidiol can activate TRPV4 (Oláh et al., 2014) and suggesting the presence of functional TRPV4 channels in human podocytes.

To further dissect the functionality of TRPV4, we investigated the effect of the hyper-potent TRPV4 agonist, GSK1016790A (Thorneloe et al., 2008) on the intracellular Ca^{2+} concentration of podocytes. We found that GSK1016790A applied at nM concentration induced a rapid and robust elevation of intracellular Ca^{2+} concentration which was strongly inhibited by the TRPV4 selective blocker, HC067047 (EC50s were found 3.63±0.33 and 57.07±6.02 nM in the absence and presence of 1 μM HC067047, respectively - Figure 4A-B). Not only the peak, but also the slope of the Ca^{2+}-transients increased dose-dependently by GSK1016790A in Ca^{2+} containing buffer even after the saturation of the Ca^{2+} signals clearly indicating higher open probability of plasma membrane located TRPV4 channels (Figure 4C-D). GSK1016790A was found to be able to elevate the intracellular Ca^{2+} even in the absence of extracellular Ca^{2+}, although it was less potent (EC50=10.04±0.72 nM) and definitely slower than in normal, Ca^{2+} buffer (Figure 4A-D), suggesting that functional TRPV4 channels are expressed on the intracellular Ca^{2+} stores, as well. However the much steeper rising phase in the presence of extracellular Ca^{2+} suggested that the majority of the channels are activated by the agonist in the plasma membrane (Figure 4D). The classical TRPV4 agonist 4α-PDD (Watanabe et al., 2002) also evoked an elevation in the intracellular Ca^{2+} concentration (EC50=0.52±0.06 μM) and its effect was also inhibited by HC067047, although 4α-PDD was found less effective than GSK1016790A (Figure 4E-F). 4α-PDD evoked responses were abolished in the absence of extracellular Ca^{2+} suggesting again that the majority of the activated TRPV4 channels are located in the plasma membrane. This was also supported by whole cell patch clamp experiments in which we have detected strong GSK1016790A induced transmembrane currents which biophysical characteristic corresponded to TRPV4. Similarly

to the Ca^{2+} signals, GSK1016790A induced transmembrane currents were also inhibited by HC067047 (Figure 4G-H).

Since specific agonist and antagonists are not available commercially, the pharmacological identification and separation of TRPV3 is the most challenging among heat sensitive TRPV channels. Although they lack specificity, several herbal compounds, like eugenol, thymol or carvacrol, are reported as potent TRPV3 activators (Xu et al., 2006; Vriens et al., 2008). Probing these compounds on differentiated human podocytes we found a marked activation in the concentration range reported for effective activation of TRPV3 (Xu et al., 2006; Vriens et al., 2008), suggesting the presence of functional TRPV3 on human podocytes (Figure 5A-B.). However, the dose-response relationships were not saturated up to 1.5 mM and did not show sigmoid shape, suggesting that these compounds can activate other targets on podocytes, as well. In contrast, application of 2-APB, a synthetic but also not specific activator of TRPV3 (Chung et al., 2004; Vriens et al., 2009), significantly elevated cytoplasmic Ca^{2+} concentration from extracellular source resulting in a sigmoidal dose-response relationship (EC50=499.51±51.166 µM) (Figure 5C-D). Although the above compounds are effective activators of TRPV3, all of them lack specificity and can affect cytoplasmic Ca^{2+} concentration via several other targets including other TRP channels, store operated Ca^{2+} entry or inositol trisphosphate (IP_3) receptors. Selected concentrations of carvacrol, thymol and 2-APB were only partially inhibited by the general, non-specific TRP channel inhibitor ruthenium red (≤35% inhibition); likewise, the endogenous TRPV3 inhibitor IPP (Bang et al., 2011) partially inhibited only the 2-APB induced Ca^{2+} transients (~23% inhibition) (Figure 5E). Transfection of the podocytes with siRNA targeting TRPV3 resulted in a marked decrease in the expression of the channel compared to the scrambled RNA transfected control cells (Figure 5F). Although the TRPV3 silencing was found effective, it does not influenced the Ca^{2+} responses evoked by the above agonists. These results indicate that although TRPV3 activators were effective in increasing cytoplasmic Ca^{2+} concentration of differentiated human podocytes, their application likely evokes several off-target effects and the contribution of TRPV3 to these Ca^{2+} responses is minimal.

Discussion

In our current study, we provided the first evidence for the functional expression of the heat sensitive members of the vanilloid subfamily of TRP channels in human podocytes. We described heat evoked Ca^{2+} signals and detected the presence of TRPV1, 2, 3 and 4 proteins in the investigated conditionally immortalized human podocyte cell line. However, native TRPV3 and TRPV4 were detected at lower molecular weight in podocytes compared to the recombinant channels, which might suggest different degradation of these channels in the two cell lines. Quantitative analysis of the mRNA transcripts revealed that TRPV1 and TRPV4 are the dominantly expressed TRPV channels but TRPV2 and TRPV3 were also detected at lower levels. These findings are highly consistent with publicly available microarray data of Da Sacco et al., (2013) (GEO Series accession number: GSE49439). Moreover, an additional transcriptome analysis (Boerries et al., 2013) also detected TRPV1-4 transcripts in primary isolated mouse podocytes.

Dissecting the functionality of TRPVs, we surprisingly found that TRPV1 specific agonist capsaicin and the ultrapotent agonist RTX failed to induce significant Ca^{2+} entry to podocytes suggesting loss of vanilloid sensitivity or an impaired functionality of TRPV1 in the investigated cell line. TRPV1, earlier assigned as capsaicin-receptor, is robustly activated by capsaicin in human and rodents, however TRPV1 was found insensitive for capsaicin in several other species (Jordt and Julius, 2002; Gavva et al., 2004). Recent research revealed the molecular mechanism of capsaicin binding to TRPV1 and identified key amino acid residues in which mutations decreased capsaicin sensitivity (Yang et al., 2015). Single nucleotide polymorphisms in the human TRPV1 are also known to be associated with lowered capsaicin sensitivity (Cantero-Recasens et al., 2010). Moreover, a capsaicin insensitive splice variant TRPV1b was identified and its expression was reported in trigeminal and dorsal root ganglia (Lu et al., 2005; Charrua et al., 2008; Mistry et al., 2014) and in keratinocytes (Pecze et al., 2008). If TRPV1b is co-expressed with TRPV1 it behaves as dominant negative subunit disrupting capsaicin/vanilloid sensitivity of the channel (Vos et al., 2006). In our case, both mutations in the key residues or the presence of the dominant negative subunit TRPV1b can be a rational explanation for the finding that in spite of the molecular expression of TRPV1, we did not find any functional effect of capsaicin. Although desensitization by signaling pathways or functional inhibition by interacting partners, e.g. phosphoinositols (Planells-Cases et al., 2011; Rohacs, 2015), may also decrease the capsaicin sensitivity of TRPV1, further studies are needed to identify the contribution of the different potential mechanisms.

In contrast to TRPV1, TRPV2 was detected not only at molecular level, but the presence of functional TRPV2 channels in the membrane of cultured human podocytes is strongly supported by our results showing that TRPV2 agonist CBD induced a calcium influx from the extracellular space which was inhibited by tranilast, a suggested antagonist of TRPV2. However, the specific TRPV4 blocker HC067047 also effectively inhibited CBD induced Ca^{2+} entry; therefore we concluded that functional TRPV4 channels can also be involved in the effect of CBD. Indeed, the classical TRPV4 agonist 4-αPDD and the ultrapotent GSK1016790A induced a fast and robust increase in the cytoplasmic Ca^{2+} concentration which was strongly inhibited in the presence of the antagonist HC067047. In podocytes, GSK1016790A also induced marked transmembrane currents with a voltage dependence characteristic for TRPV4 (Jin et al., 2011) and blocked by HC067047. These functional results suggest that, in good accordance with the molecular expression data, TRPV4 is the dominantly expressed thermosensitive TRPV channel in human podocytes.

In contrast to TRPV4, the functional presence of TRPV3 is ambiguous. Although we identified the presence of TRPV3 proteins, quantitative analysis of expression of TRPV3 transcripts suggested a relatively low expression level compared to TRPV4. The pharmacological identification is uncertain since we lack commercially available, effective and highly specific TRPV3 agonists and antagonists. The botanical compounds carvacrol, thymol and eugenol, as well as the synthetic 2-APB used in our experiments are potent, but highly unspecific agonists generally used to study TRPV3 functions (Chung et al., 2004; Xu et al., 2006; Vriens et al., 2008, 2009). In human podocytes, all the above compounds evoked marked elevation of the cytoplasmic Ca^{2+} concentration, which source was mainly the extracellular space (at least if compounds were applied at concentrations ≤1 mM), but only the effect of 2-APB was saturated in the concentration range applied making possible the correct fitting of a sigmoidal dose-response curve. The experimentally determined EC50 (~500 µM) was higher, than found earlier in electrophysiological studies on recombinant TRPV3 (~42 µM at physiological membrane potential - Chung et al., 2004). Moreover, the general TRP channel blocker ruthenium red (Alexander et al., 2015) could only partially block the effect of the compounds and the endogenous TRPV3 inhibitor IPP was effective partially blocking only 2-APB evoked Ca^{2+} signals. In contrast, RNAi mediated silencing of the molecular expression of TRPV3 did not influenced the effect of the agonists. All this results argue for manifest off-target effects of the TRPV3 ligands which can include the activation of several other TRP channels, and numerous other targets involved in cellular Ca^{2+} handling, like IP_3 receptors, ryanodine receptors, sarcoplasmic reticulum Ca^{2+}-ATPase or store operated Ca^{2+} entry

mechanisms (Chung et al., 2004; Xu et al., 2006; Sárközi et al., 2007; Vriens et al., 2008, 2009; Hsu et al., 2011; Liang and Lu, 2012). Therefore, although our results suggest that TRPV3 is expressed in human podocytes, its functionality is not clear. The exact role of TRPV3 in the Ca^{2+} signals evoked by its activators needs further investigations. However, more specific pharmacological tools hopefully available in the near future are desired to validate our results and further dissect the potential role of TRPV3 in podocytes.

The expression of heat and mechanosensitive TRPV channels has been already being investigated in the lower urinary tract and in the kidney since their cloning (Hayes et al., 2000; Strotmann et al., 2000; Kassmann et al., 2013). Although clear evidences support the role of TRPV1 in the control of lower urinary tract functions, its expression in urothelial cells is still under debate (for a review see: Franken et al., 2014). TRPV4 is more abundantly expressed in the non-neural cells of the urinary tract. In the kidney, TRPV4 expression was found overall in the constitutively water impermeable segments of the nephron (thin and thick ascending limb, distal convoluted tubule) and in the collecting ducts, as well (Tian et al., 2004). Moreover, both TRPV1 and TRPV4 were described to form functionally active channels in the endothelium of the renal vasculature (Chen et al., 2015).

Although the expression of heat sensitive TRPV channels is known in the kidney, we lack the complete understanding of their functions in the different segments of the tubular epithelium, and we especially lack any data regarding podocytes. Although actually we do not have data about the physiological role of TRPV1-4 in regulating cellular functions of podocytes, it is well known, that Ca^{2+} signaling related to other TRP channels, namely TRPC6 and TRPC5, have a crucial impact on podocytes' biological functions influencing cytoskeletal rearrangements and consequently the physical characteristic of the slit diaphragm and the filtration barrier. Interestingly, TRPC5 and TRPC6 seem to oppositely regulate podocyte actin dynamics and cell motility via RhoA and Rac1, respectively (Tian et al., 2010; Schaldecker et al., 2013; Tian and Ishibe, 2016). Moreover, a recent study suggested that wild type TRPC6, but not the mutant allele TRPC6-N143S, originally described in a family with FSGS, showed intrinsic mechanosensitivity and responded to hypotonic challenges (Wilson and Dryer, 2014) suggesting a potential role of osmotic stimuli and consequent (TRP mediated) Ca^{2+} signals in the regulation of podocytes' functions.

In the renal tubular system, an important role in transmitting the effect of tubular flow and osmolarity is attributed to TRPV4 (Mamenko et al., 2015). TRPV4 mediated flow-induced increases in intracellular Ca^{2+} concentration in medullary thick ascending limbs (Cabral et al., 2015) and its role was revealed in hypotonic stimuli induced Ca^{2+} entry needed for regulatory

volume decrease in renal cortical collecting duct cells (Galizia et al., 2012). Beyond osmosensation, TRPV4 seems to play an emerging role in the formation of epithelial barrier in several tissues. In airway epithelium, sheer stress enhanced epithelial barrier function via serial activation of TRPV4 and voltage gated L-type Ca^{2+} channels (Sidhaye et al., 2008). In epidermal keratinocytes of the skin, functionally active TRPV4 channels were found to interact with adherent junction proteins and actin cytoskeleton, enhancing cell-cell junction and tight barrier formation. In this process TRPV4 contributed to the elevation of intracellular Ca^{2+} concentration resulting in small GTPase Rho activation and consequent actin rearrangement. Moreover, its pharmacological activation augmented tight junction development and barrier recovery (Sokabe et al., 2010; Kida et al., 2012; Akazawa et al., 2013). Most recently, TRPV4 was described in bladder urothelium and kidney collecting duct epithelium associating with adherent junctions directly interacting with junctional proteins, especially α-catenin, an intracellular adherent junction protein connected to the actin cytoskeleton (Janssen et al., 2016). All these data further suggest a putative contribution of TRPV4 to the fine orchestration of podocytes Ca^{2+} homeostasis regulating the filtration barrier.

Since podocytes in the outermost layer of the glomeruli form the final barrier to protein loss, their injury is often associated with marked proteinuria syndromes (Somlo and Mundel, 2000). Distinct diseases, like diabetic nephropathy, hypertension, as well as inherited or drug-induced podocytopathies can results in disruption of the slit diaphragm leading to proteinuria (Mathieson, 2011).. Although the detailed pathomechanism is still unknown, cytoskeletal disorganization as a consequence of the altered Ca^{2+} signaling can be an important step. Although the potential role of TRPV channels has not been investigated yet, numerous studies suggested the role of several elements of the cellular Ca^{2+} signaling pathways like TRPC6 or angiotensin II receptor related pathways (Wieder and Greka, 2016). The activity of the TRPV channels, especially TRPV4, can be affected directly by the altered, disease associated physical environment like increased flow and shear stress or altered osmotic concentrations, as detailed above. However, TRPV4 can be modulated by intracellular signaling pathways, among else, by angiotensin II signaling (Shukla et al., 2010; Tajada et al., 2017) which is of particular importance in podocytes (Hoffmann et al., 2004). These potential integrative role of the TRPV(4) channels can make them especially appealing targets for future drug developments in various forms of podocyte associated diseases.

All in all, although further studies are needed to clarify the potential role of TRPV channels in podocyte (patho)physiology, detailed understanding of their pharmacological role

in physiological and disease conditions might contribute to the development of future therapies of primary and secondary podocytopathies and related kidney diseases.

Author contributions

LA, BIT and BK designed and performed the experiments and collected and analyzed the data. TSZ and TB designed and managed the research study. LA, BIT and TB wrote the paper which was carefully edited and reviewed by all other authors.

Acknowledgments

The presented work was supported through the New National Excellence Program of the Ministry of Human Capacities and by Hungarian research grants OTKA 76065, NKFI K_16 120187, NKFI K_16 120552, TÁMOP-4.2.2.A-11/1/KONV-2012-0045, and LP003-2011/2015. BIT is a recipient of the János Bolyai research scholarship of the Hungarian Academy of Sciences.

Conflict of interest

Authors declare no conflicts of interest.

References

Akazawa Y, Yuki T, Yoshida H, Sugiyama Y and Inoue S (2013). Activation of TRPV4 strengthens the tight-junction barrier in human epidermal keratinocytes. Skin Pharmacol Physiol *26*: 15–21.

Alexander SP, Catterall WA, Kelly E, Marrion N, Peters JA, Benson HE, et al. (2015). The Concise Guide to PHARMACOLOGY 2015/16: Voltage-gated ion channels. Br J Pharmacol *172*: 5904–5941.

Alvarez DF, King JA, Weber D, Addison E, Liedtke W and Townsley MI (2006). Transient Receptor Potential Vanilloid 4–Mediated Disruption of the Alveolar Septal Barrier A Novel Mechanism of Acute Lung Injury. Circ Res *99*: 988–995.

Ambrus L, Oláh A, Oláh T, Balla G, Saleem MA, Orosz P, et al. (2015). Inhibition of TRPC6 by protein kinase C isoforms in cultured human podocytes. J Cell Mol Med *19*: 2771–2779.

Bang S, Yoo S, Yang T-J, Cho H and Hwang SW (2011). Isopentenyl pyrophosphate is a novel antinociceptive substance that inhibits TRPV3 and TRPA1 ion channels. Pain *152*: 1156–1164.

Boerries M, Grahammer F, Eiselein S, Buck M, Meyer C, Goedel M, et al. (2013). Molecular fingerprinting of the podocyte reveals novel gene and protein regulatory networks. Kidney Int *83*: 1052–1064.

Cabral PD, Capurro C and Garvin JL (2015). TRPV4 mediates flow-induced increases in intracellular Ca in medullary thick ascending limbs. Acta Physiol Oxf Engl *214*: 319–328.

Cantero-Recasens G, Gonzalez JR, Fandos C, Duran-Tauleria E, Smit LAM, Kauffmann F, et al. (2010). Loss of function of transient receptor potential vanilloid 1 (TRPV1) genetic variant is associated with lower risk of active childhood asthma. J Biol Chem *285*: 27532–27535.

Caterina MJ, Schumacher MA, Tominaga M, Rosen TA, Levine JD and Julius D (1997). The capsaicin receptor: a heat-activated ion channel in the pain pathway. Nature *389*: 816–824.

Charrua A, Reguenga C, Paule CC, Nagy I, Cruz F and Avelino A (2008). Cystitis is associated with TRPV1b-downregulation in rat dorsal root ganglia. Neuroreport *19*: 1469–1472.

Chen L, Kaßmann M, Sendeski M, Tsvetkov D, Marko L, Michalick L, et al. (2015). Functional transient receptor potential vanilloid 1 and transient receptor potential vanilloid 4 channels along different segments of the renal vasculature. Acta Physiol Oxf Engl *213*: 481–491.

Chung M-K, Lee H, Mizuno A, Suzuki M and Caterina MJ (2004). 2-aminoethoxydiphenyl borate activates and sensitizes the heat-gated ion channel TRPV3. J Neurosci *24*: 5177–5182.

Curtis MJ, Bond RA, Spina D, Ahluwalia A, Alexander SPA, Giembycz MA, et al. (2015). Experimental design and analysis and their reporting: new guidance for publication in BJP. Br J Pharmacol *172*: 3461–3471.

Da Sacco S, Lemley KV, Sedrakyan S, Zanusso I, Petrosyan A, Peti-Peterdi J, et al. (2013). A novel source of cultured podocytes. PloS One *8*: e81812.

De Petrocellis L, Orlando P, Moriello AS, Aviello G, Stott C, Izzo AA, et al. (2012). Cannabinoid actions at TRPV channels: effects on TRPV3 and TRPV4 and their potential relevance to gastrointestinal inflammation. Acta Physiol Oxf Engl *204*: 255–266.

Dimke H, Hoenderop JGJ and Bindels RJM (2011). Molecular basis of epithelial Ca2+ and Mg2+ transport: insights from the TRP channel family. J Physiol *589*: 1535–1542.

Dryer SE, and Reiser J (2010). TRPC6 channels and their binding partners in podocytes: role in glomerular filtration and pathophysiology. Am J Physiol Renal Physiol *299*: F689-701.

Earley S, and Brayden JE (2015). Transient receptor potential channels in the vasculature. Physiol Rev *95*: 645–690.

Everaerts W, Zhen X, Ghosh D, Vriens J, Gevaert T, Gilbert JP, et al. (2010). Inhibition of the cation channel TRPV4 improves bladder function in mice and rats with cyclophosphamide-induced cystitis. Proc Natl Acad Sci U S A *107*: 19084–19089.

Feng N-H, Lee H-H, Shiang J-C and Ma M-C (2008). Transient receptor potential vanilloid type 1 channels act as mechanoreceptors and cause substance P release and sensory activation in rat kidneys. Am J Physiol Renal Physiol *294*: F316-325.

Franken J, Uvin P, De Ridder D and Voets T (2014). TRP channels in lower urinary tract dysfunction. Br J Pharmacol *171*: 2537–2551.

Galizia L, Pizzoni A, Fernandez J, Rivarola V, Capurro C and Ford P (2012). Functional interaction between AQP2 and TRPV4 in renal cells. J Cell Biochem *113*: 580–589.

Gavva NR, Klionsky L, Qu Y, Shi L, Tamir R, Edenson S, et al. (2004). Molecular determinants of vanilloid sensitivity in TRPV1. J Biol Chem *279*: 20283–20295.

Grace MS, Baxter M, Dubuis E, Birrell MA and Belvisi MG (2014). Transient receptor potential (TRP) channels in the airway: role in airway disease. Br J Pharmacol *171*: 2593–2607.

Hayes P, Meadows HJ, Gunthorpe MJ, Harries MH, Duckworth DM, Cairns W, et al. (2000). Cloning and functional expression of a human orthologue of rat vanilloid receptor-1. Pain *88*: 205–215.

Hisanaga E, Nagasawa M, Ueki K, Kulkarni RN, Mori M and Kojima I (2009). Regulation of calcium-permeable TRPV2 channel by insulin in pancreatic beta-cells. Diabetes *58*: 174–184.

Hsu S-S, Lin K-L, Chou C-T, Chiang A-J, Liang W-Z, Chang H-T, et al. (2011). Effect of thymol on Ca2+ homeostasis and viability in human glioblastoma cells. Eur J Pharmacol *670*: 85–91.

Janssen D a. W, Jansen CJF, Hafmans TG, Verhaegh GW, Hoenderop JG, Heesakkers JPFA, et al. (2016). TRPV4 channels in the human urogenital tract play a role in cell junction formation and epithelial barrier. Acta Physiol Oxf Engl *218*: 38–48.

Jordt S-E, and Julius D (2002). Molecular basis for species-specific sensitivity to 'hot' chili peppers. Cell *108*: 421–430.

Kassmann M, Harteneck C, Zhu Z, Nürnberg B, Tepel M and Gollasch M (2013). Transient receptor potential vanilloid 1 (TRPV1), TRPV4, and the kidney. Acta Physiol Oxf Engl *207*: 546–564.

Kida N, Sokabe T, Kashio M, Haruna K, Mizuno Y, Suga Y, et al. (2012). Importance of transient receptor potential vanilloid 4 (TRPV4) in epidermal barrier function in human skin keratinocytes. Pflüg Arch Eur J Physiol *463*: 715–725.

Liang WZ, and Lu CH (2012). Carvacrol-induced [Ca2+]i rise and apoptosis in human glioblastoma cells. Life Sci *90*: 703–711.

Lu G, Henderson D, Liu L, Reinhart PH and Simon SA (2005). TRPV1b, a functional human vanilloid receptor splice variant. Mol Pharmacol *67*: 1119–1127.

Mamenko M, Zaika O, Boukelmoune N, O'Neil RG and Pochynyuk O (2015). Deciphering physiological role of the mechanosensitive TRPV4 channel in the distal nephron. Am J Physiol Renal Physiol *308*: F275-286.

Mathieson PW (2011). The podocyte as a target for therapies--new and old. Nat Rev Nephrol *8*: 52–56.

Mihara H, Boudaka A, Shibasaki K, Yamanaka A, Sugiyama T and Tominaga M (2010). Involvement of TRPV2 activation in intestinal movement through nitric oxide production in mice. J Neurosci *30*: 16536–16544.

Mistry S, Paule CC, Varga A, Photiou A, Jenes A, Avelino A, et al. (2014). Prolonged exposure to bradykinin and prostaglandin E2 increases TRPV1 mRNA but does not alter TRPV1 and TRPV1b protein expression in cultured rat primary sensory neurons. Neurosci Lett *564*: 89–93.

Moran MM, McAlexander MA, Bíró T and Szallasi A (2011). Transient receptor potential channels as therapeutic targets. Nat Rev Drug Discov *10*: 601–620.

Nie L, Oishi Y, Doi I, Shibata H and Kojima I (1997). Inhibition of proliferation of MCF-7 breast cancer cells by a blocker of Ca(2+)-permeable channel. Cell Calcium *22*: 75–82.

Nilius B, and Szallasi A (2014). Transient receptor potential channels as drug targets: from the science of basic research to the art of medicine. Pharmacol Rev *66*: 676–814.

Oláh A, Tóth BI, Borbíró I, Sugawara K, Szöllõsi AG, Czifra G, et al. (2014). Cannabidiol exerts sebostatic and antiinflammatory effects on human sebocytes. J Clin Invest *124*: 3713–3724.

Pecze L, Szabó K, Széll M, Jósvay K, Kaszás K, Kúsz E, et al. (2008). Human keratinocytes are vanilloid resistant. PloS One *3*: e3419.

Perálvarez-Marín A, Doñate-Macian P and Gaudet R (2013). What do we know about the transient receptor potential vanilloid 2 (TRPV2) ion channel? FEBS J *280*: 5471–5487.

Planells-Cases R, Valente P, Ferrer-Montiel A, Qin F and Szallasi A (2011). Complex regulation of TRPV1 and related thermo-TRPs: implications for therapeutic intervention. Adv Exp Med Biol *704*: 491–515.

Qin N, Neeper MP, Liu Y, Hutchinson TL, Lubin ML and Flores CM (2008). TRPV2 is activated by cannabidiol and mediates CGRP release in cultured rat dorsal root ganglion neurons. J Neurosci *28*: 6231–6238.

Retailleau K, and Duprat F (2014). Polycystins and partners: proposed role in mechanosensitivity. J Physiol *592*: 2453–2471.

Rohacs T (2015). Phosphoinositide regulation of TRPV1 revisited. Pflüg Arch Eur J Physiol *467*: 1851–1869.

Saleem MA, O'Hare MJ, Reiser J, Coward RJ, Inward CD, Farren T, et al. (2002). A conditionally immortalized human podocyte cell line demonstrating nephrin and podocin expression. J Am Soc Nephrol JASN *13*: 630–638.

Sárközi S, Almássy J, Lukács B, Dobrosi N, Nagy G and Jóna I (2007). Effect of natural phenol derivatives on skeletal type sarcoplasmic reticulum Ca2+ -ATPase and ryanodine receptor. J Muscle Res Cell Motil *28*: 167–174.

Schaldecker T, Kim S, Tarabanis C, Tian D, Hakroush S, Castonguay P, et al. (2013). Inhibition of the TRPC5 ion channel protects the kidney filter. J Clin Invest *123*: 5298–5309.

Schindelin J, Arganda-Carreras I, Frise E, Kaynig V, Longair M, Pietzsch T, et al. (2012). Fiji: an open-source platform for biological-image analysis. Nat Methods *9*: 676–682.

Schindelin J, Rueden CT, Hiner MC and Eliceiri KW (2015). The ImageJ ecosystem: An open platform for biomedical image analysis. Mol Reprod Dev *82*: 518–529.

Shukla AK, Kim J, Ahn S, Xiao K, Shenoy SK, Liedtke W, et al. (2010). Arresting a transient receptor potential (TRP) channel: beta-arrestin 1 mediates ubiquitination and functional down-regulation of TRPV4. J Biol Chem *285*: 30115–30125.

Sidhaye VK, Schweitzer KS, Caterina MJ, Shimoda L and King LS (2008). Shear stress regulates aquaporin-5 and airway epithelial barrier function. Proc Natl Acad Sci U S A *105*: 3345–3350.

Sokabe T, Fukumi-Tominaga T, Yonemura S, Mizuno A and Tominaga M (2010). The TRPV4 channel contributes to intercellular junction formation in keratinocytes. J Biol Chem *285*: 18749–18758.

Somlo S, and Mundel P (2000). Getting a foothold in nephrotic syndrome. Nat Genet *24*: 333–335.

Southan C, Sharman JL, Benson HE, Faccenda E, Pawson AJ, Alexander SP et al. (2016). The IUPHAR/BPS Guide to PHARMACOLOGY in 2016: towards curated quantitative interactions between 1300 protein targets and 6000 ligands. Nucl Acids Res *44*: D1054-1068.

Strotmann R, Harteneck C, Nunnenmacher K, Schultz G and Plant TD (2000). OTRPC4, a nonselective cation channel that confers sensitivity to extracellular osmolarity. Nat Cell Biol *2*: 695–702.

Tajada S, Moreno CM, O'Dwyer S, Woods S, Sato D, Navedo MF, et al. (2017). Distance constraints on activation of TRPV4 channels by AKAP150-bound PKCα in arterial myocytes. J Gen Physiol *149*: 639–659.

Thorneloe KS, Sulpizio AC, Lin Z, Figueroa DJ, Clouse AK, McCafferty GP, et al. (2008). N-((1S)-1-{[4-((2S)-2-{[(2,4-dichlorophenyl)sulfonyl]amino}-3-hydroxypropanoyl)-1-piperazinyl]carbonyl}-3-methylbutyl)-1-benzothiophene-2-carboxamide (GSK1016790A), a novel and potent transient receptor potential vanilloid 4 channel agonist induces urinary bladder contraction and hyperactivity: Part I. J Pharmacol Exp Ther *326*: 432–442.

Tian D, Jacobo SMP, Billing D, Rozkalne A, Gage SD, Anagnostou T, et al. (2010). Antagonistic regulation of actin dynamics and cell motility by TRPC5 and TRPC6 channels. Sci Signal *3*: ra77.

Tian W, Salanova M, Xu H, Lindsley JN, Oyama TT, Anderson S, et al. (2004). Renal expression of osmotically responsive cation channel TRPV4 is restricted to water-impermeant nephron segments. Am J Physiol Renal Physiol *287*: F17-24.

Tian X, and Ishibe S (2016). Targeting the podocyte cytoskeleton: from pathogenesis to therapy in proteinuric kidney disease. Nephrol Dial Transplant Off Publ Eur Dial Transpl Assoc - Eur Ren Assoc.

Tóth BI, and Nilius B (2015). Chapter 2 - Transient Receptor Potential Dysfunctions in Hereditary Diseases: TRP Channelopathies and Beyond A2 - Szallasi, Arpad. In TRP Channels as Therapeutic Targets, (Boston: Academic Press), pp 13–33.

Tóth BI, Oláh A, Szöllősi AG and Bíró T (2014). TRP channels in the skin. Br J Pharmacol *171*: 2568–2581.

Vos MH, Neelands TR, McDonald HA, Choi W, Kroeger PE, Puttfarcken PS, et al. (2006). TRPV1b overexpression negatively regulates TRPV1 responsiveness to capsaicin, heat and low pH in HEK293 cells. J Neurochem *99*: 1088–1102.

Vriens J, Appendino G and Nilius B (2009). Pharmacology of vanilloid transient receptor potential cation channels. Mol Pharmacol *75*: 1262–1279.

Vriens J, Nilius B and Vennekens R (2008). Herbal Compounds and Toxins Modulating TRP Channels. Curr Neuropharmacol *6*: 79–96.

Watanabe H, Davis JB, Smart D, Jerman JC, Smith GD, Hayes P, et al. (2002). Activation of TRPV4 channels (hVRL-2/mTRP12) by phorbol derivatives. J Biol Chem *277*: 13569–13577.

Wieder N, and Greka A (2016). Calcium, TRPC channels, and regulation of the actin cytoskeleton in podocytes: towards a future of targeted therapies. Pediatr Nephrol Berl Ger *31*: 1047–1054.

Wilson C, and Dryer SE (2014). A mutation in TRPC6 channels abolishes their activation by hypoosmotic stretch but does not affect activation by diacylglycerol or G protein signaling cascades. Am J Physiol Renal Physiol *306*: F1018-1025.

Woudenberg-Vrenken TE, Bindels RJM and Hoenderop JGJ (2009). The role of transient receptor potential channels in kidney disease. Nat Rev Nephrol *5*: 441–449.

Xu H, Delling M, Jun JC and Clapham DE (2006). Oregano, thyme and clove-derived flavors and skin sensitizers activate specific TRP channels. Nat Neurosci *9*: 628–635.

Yang D, Luo Z, Ma S, Wong WT, Ma L, Zhong J, et al. (2010). Activation of TRPV1 by dietary capsaicin improves endothelium-dependent vasorelaxation and prevents hypertension. Cell Metab *12*: 130–141.

Yang F, Xiao X, Cheng W, Yang W, Yu P, Song Z, et al. (2015). Structural mechanism underlying capsaicin binding and activation of the TRPV1 ion channel. Nat Chem Biol *11*: 518–524.

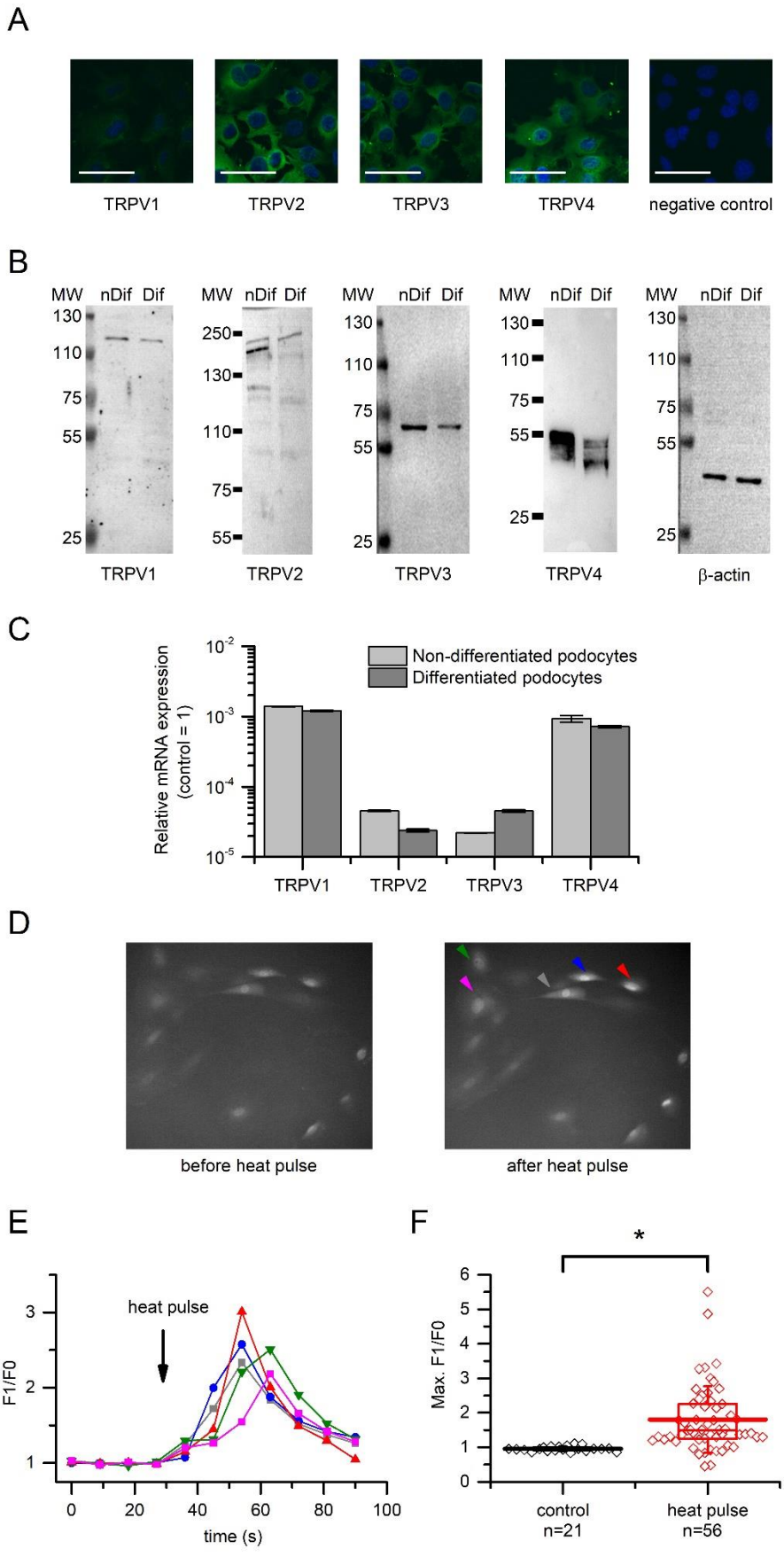

Figure 1:

Expression of thermosensitive transient receptor potential vanilloid 1-4 (TRPV1-4) channels in differentiated human podocytes. (A) TRPV1-4 immunoreactivity were determined on differentiated human podocyte cultures by fluorescent labeling (Alexa-Fluor®-488, green fluorescence). Nuclei were counterstained with DAPI (blue fluorescence). Calibration mark: 50 µm. (B) Lysates of non-differentiated (nDif) and differentiated (Dif) human podocytes were subjected to western blot analysis and immunolabeled with specific TRPV antibodies. To assess equal loading of protein samples, expression of β-actin was determined. MW indicates molecular weight in kDa. (C) Expression of TRPV1-4 mRNA transcripts were detected by Q-PCR in non-differentiated and differentiated human podocytes. Expression of peptidylprolyl isomerase A (cyclophilin A; PPIA), β-actin (ACTB) and glyceraldehyde 3-phosphate dehydrogenase (GAPDH) were determined and the geometrical mean of their expression was used as internal control for normalization. Data are expressed as mean ± SEM, n=3 independent determinations. (D) Representative images illustrating the effect of a heat pulse on differentiated podocytes. Cells were uploaded with the fluorescent Ca^{2+} sensitive dye Fluo-4 and challenged to a heat pulse as described in the 'Materials and methods'. Arrowheads indicate representative cells displaying increase in intracellular Ca^{2+} concentration upon heat stimulation. (E) Representative Ca^{2+} traces obtained from the experiment shown in panel (D). The colors of the traces correspond to the colors of the arrowheads in panel (D). (F) Changes in intracellular Ca^{2+} concentration in differentiated podocytes upon control and heat pulse stimulations. Markings of the box plot represents 25-50-75 percentile of the cells, thick line and whiskers indicate the mean and ±1 SD of the maximal Ca^{2+} signals, respectively. * indicates significant difference between the groups as determined by Mann-Whitney U-test, $p<0.05$.

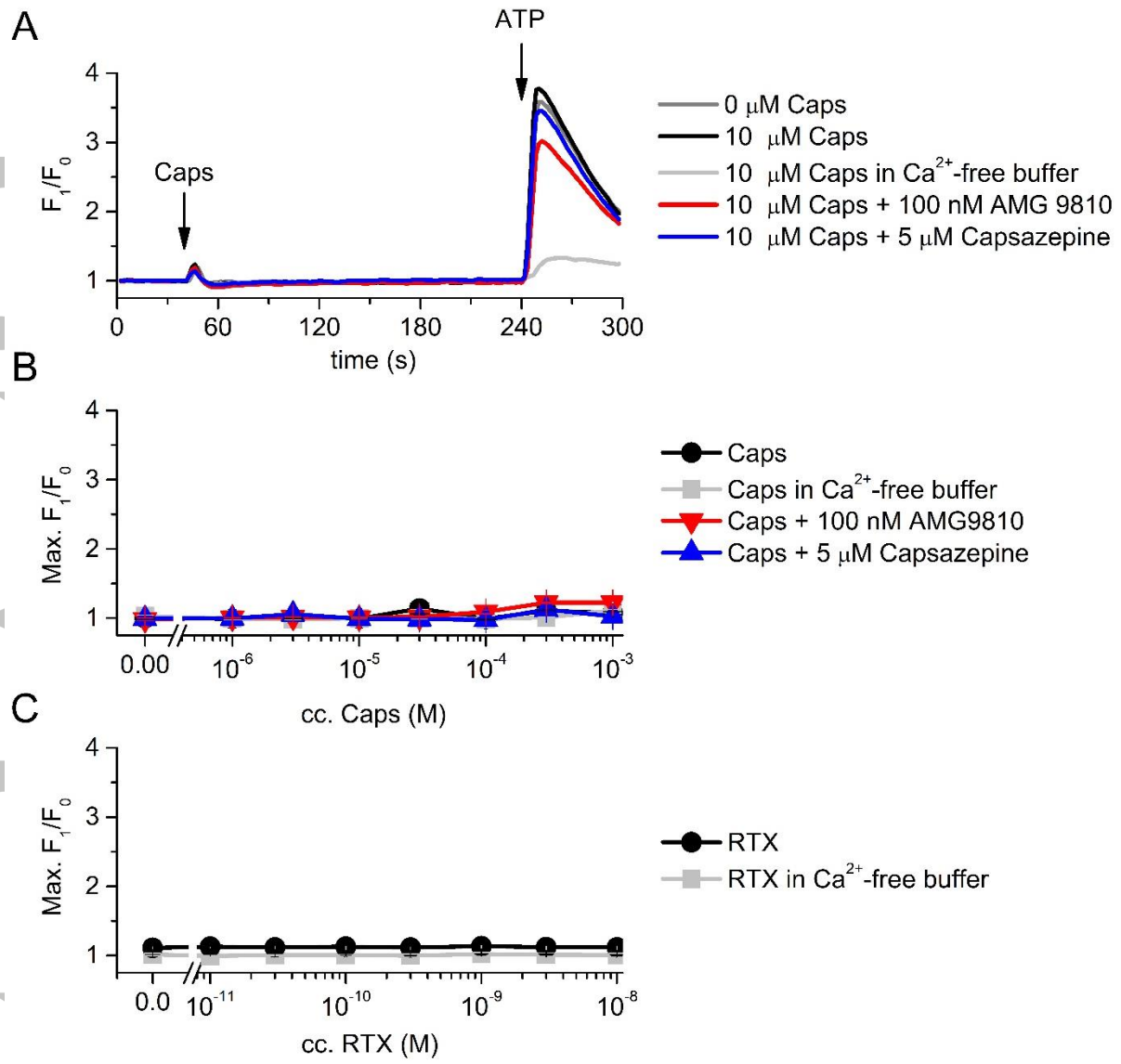

Figure 2:

Effect of TRPV1 ligands on the intracellular Ca^{2+} concentration of differentiated human podocytes. (A) Representative time curses of capsaicin application in various conditions. Cells were preincubated with capsazepine and AMG 9810 for 30 minutes and constant concentrations of the antagonists were presented as indicated on the figure continuously during the measurements. (B) Dose-response relationship of capsaicin in various conditions as indicated. The measurements were carried out as in panel A. Data are presented as mean ± SEM, n=6 in each group. (C) Dose-response relationship of RTX in normal and Ca^{2+}-free buffer. The measurements were carried out as in panel A, but RTX was applied instead of capsaicin. Data are presented as mean ± SEM, n=5 in each group.

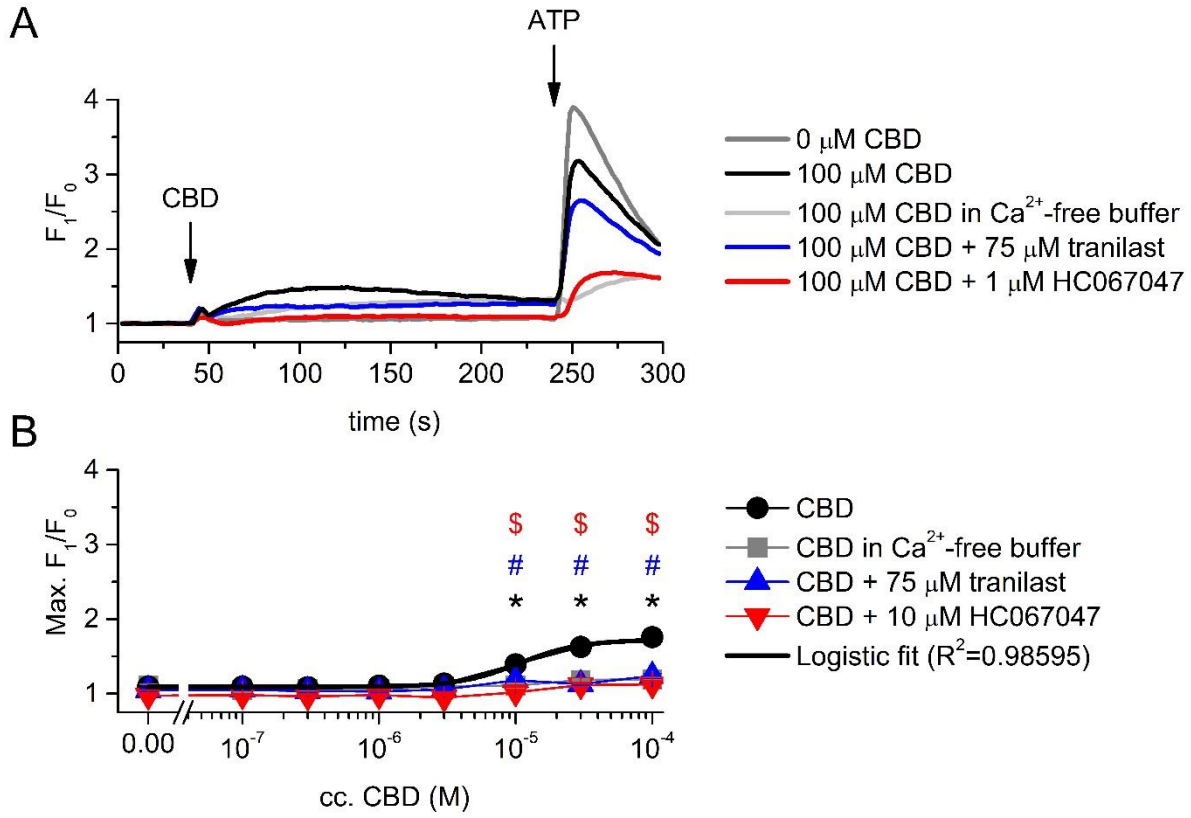

Figure 3:

Effect of CBD on the intracellular Ca^{2+} concentration of differentiated human podocytes. (A) Representative time curses of CBD applications in various conditions. Cells were preincubated with tranilast and HC067047 for 30 minutes and measurements were carried out in the continuous presence of constant antagonist concentrations as indicated on the figure. (B) Dose-response relationship of CBD in various conditions as indicated. The measurements were carried out as in panel A. Data are presented as mean ± SEM, n=6 in each group. Logistic dose-response curve fitting was carried out as described in the 'Materials and methods'. * indicates significant activation by CBD compared to the vehicle (0 μM CBD) control. # indicates significant inhibition by 75 μM tranilast. $ indicates significant inhibition by 1 μM HC067047. $P<0.05$ in each case.

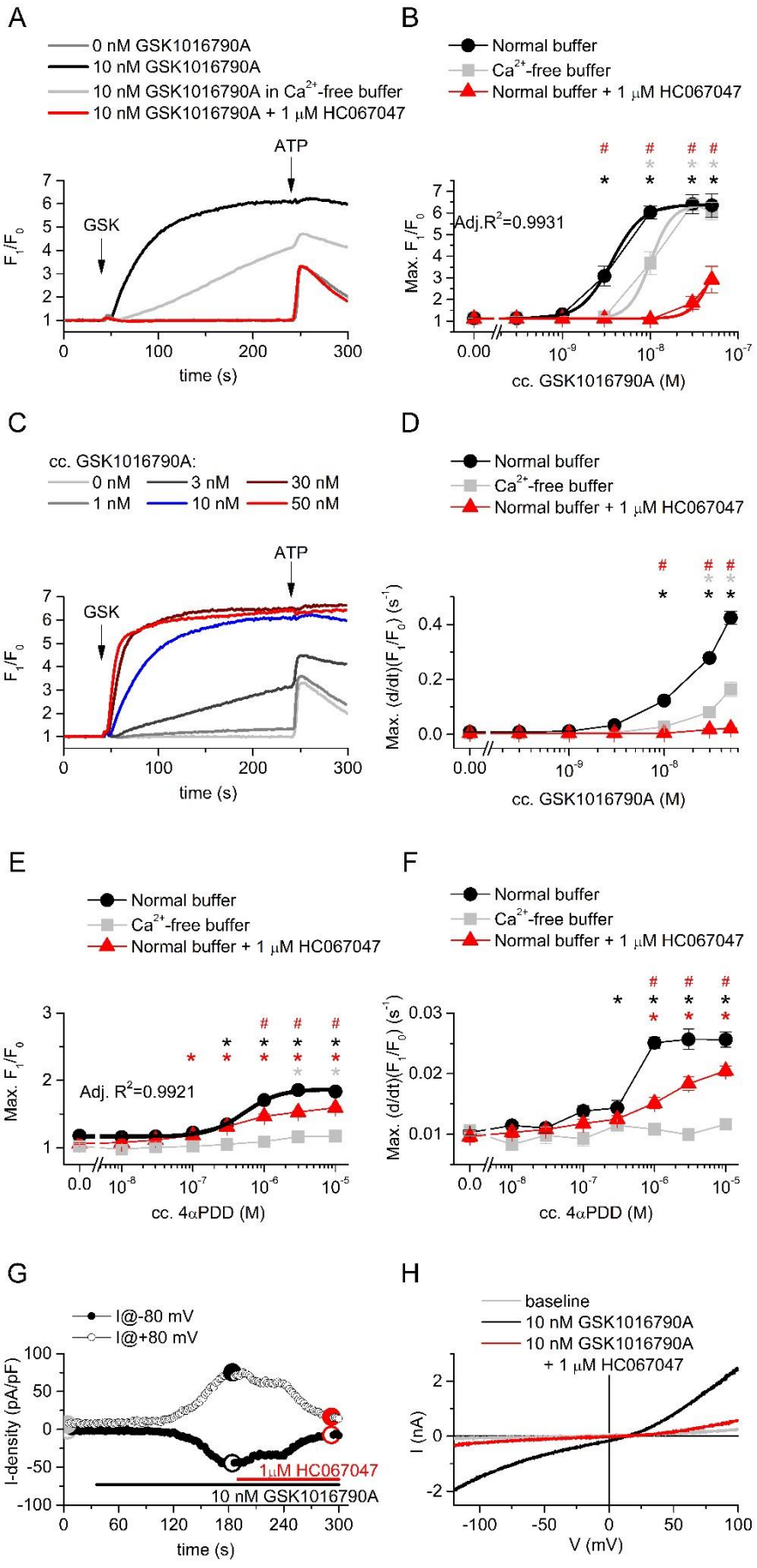

Figure 4:

Activation of TRPV4 in differentiated human podocytes. (A) Representative time courses of TRPV4 agonist GSK1016790A applications in different conditions. Cells were preincubated with HC067047 for 30 minutes and measurements were carried out in the continuous presence of constant antagonist concentrations as indicated on the figure. (B) Dose-response relationship of GSK1016790A in various conditions as indicated in the legend. Measurements were carried out as shown in panel A. Data are presented as mean ± SEM, n=6 in each group. Logistic dose-response curve was fitted as described in the 'Materials and methods' assuming equal efficacy (i.e. equal maximal responses available) in each condition. (C) Representative time courses upon application of various concentration of GSK1016790A in normal buffer illustrating the concentration dependence of the slope of the Ca^{2+} transients. (D) Concentration dependence of the maximal slope of the Ca^{2+} transients upon GSK1016790A application, n=6 in each group. (E) Dose-response relationship of 4-αPDD in various conditions as indicated in the legend. Measurements were carried out as shown in panel A, but 4- αPDD was used instead of GSK1016790A. Data are presented as mean ± SEM, n=5 in each group. Logistic dose-response curve was fitted as described in the 'Materials and methods'. (F) Concentration dependence of the maximal slope of the Ca^{2+} signals upon 4-αPDD application, n=5 in each group. (G) Representative time courses illustrating the effect of GSK1016790A and HC067047 on transmembrane currents of podocytes measured at -80 and +80 mV. A voltage ramp from -120 to +100 mV was applied at every 2 s as described in the 'Materials and methods'. (F) I-V relationship of the transmembrane currents at different time points as indicated in panel (E). In (B), (D), (E) and (F), * indicates significant activation by GSK1016790A compared to the vehicle (0 nM GSK1016790A) control in the same conditions. # indicates significant inhibition by 1 μM HC067047. $P<0.05$ in each case.

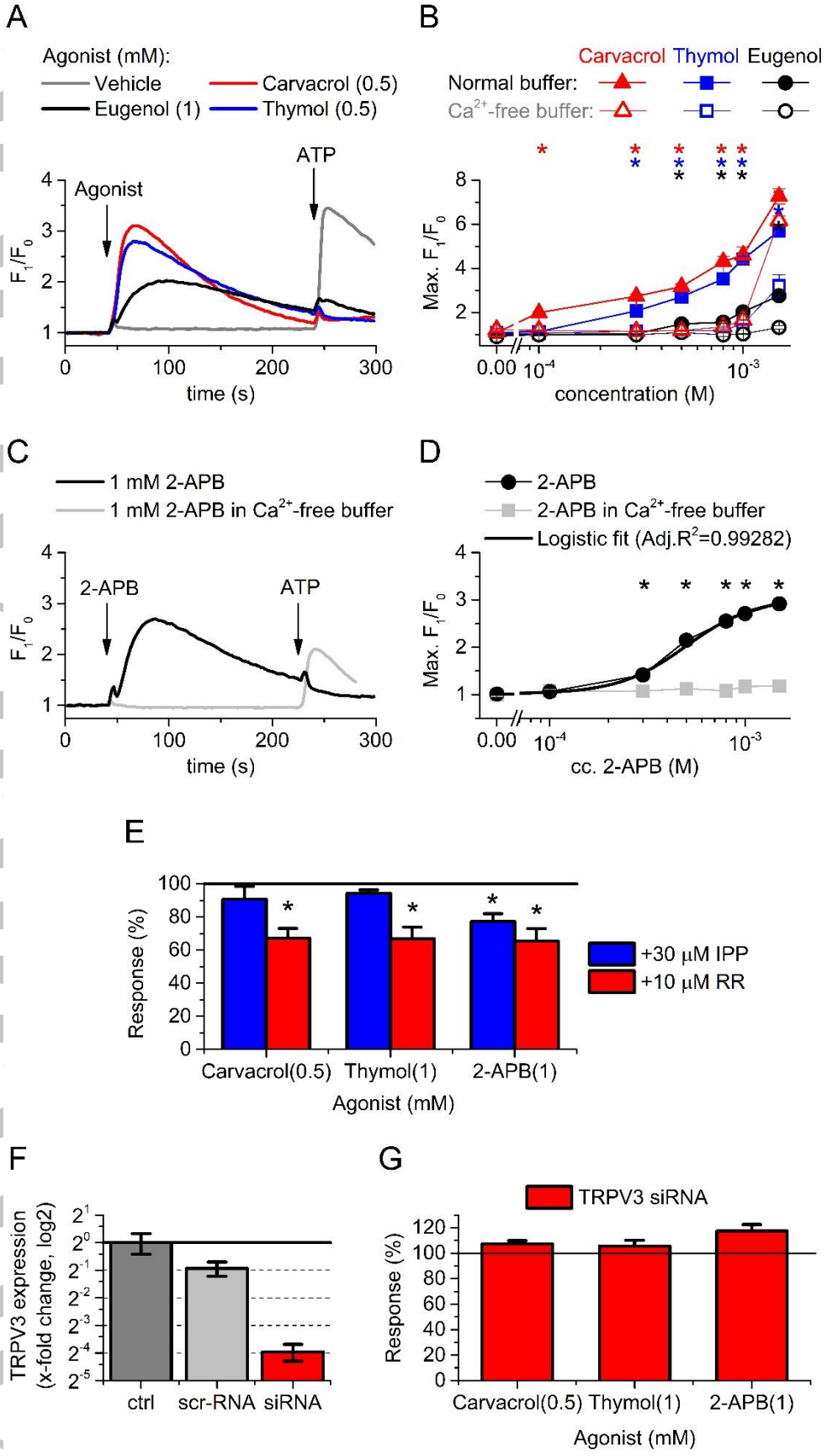

Figure 5:

Effect of TRPV3 activators on the intracellular Ca^{2+} concentration of differentiated human podocytes. (A) Representative time courses showing the application of TRPV3 activator herbal compounds on differentiated human podocytes in normal buffer. Activators and ATP as positive control were applied as shown in the figure. (B) Dose-response relationship of carvacrol, thymol and eugenol in normal and Ca^{2+}-free buffer. Measurements were carried out as shown in panel A. (C) Representative time courses showing the effect of 2-APB on differentiated human podocytes in normal and Ca^{2+}-free buffer. (D) Dose-response relationship of 2-APB treatment as shown in panel C. (B) and (D) Data are presented as mean ± SEM, n=6 in each group. * indicates significant activation by the compound marked with the corresponding color compared to the vehicle (0 µM compound) in normal buffer, $p<0.05$. (E) Effect of potential TRPV3 inhibitors ruthenium red (RR) and IPP on selected concentrations of carvacrol, thymol and 2-APB as indicated. Mean ± SEM data are presented as percent of the average of the corresponding control (i.e. agonist application in the absence of the antagonist). This normalization was performed to control the variance of the effectivity between different agonists and make comparable the inhibition evoked by the antagonists in the different groups. Response was calculated as the maximal amplitude (max. F_1/F_0-1) of the Ca^{2+} transients during the agonist application. Cells were pretreated with the inhibitors for 30 min before the agonist application and the whole experiment was carried out in the continuous presence of the inhibitors in fixed concentration. Data are presented as mean ± SEM, n=6 in each group. * indicates significant ($p<0.05$) inhibition by IPP or ruthenium red as indicated. Statistics were calculated with the raw data using ANOVA and Dunnett post-hoc test. (F) Changes in the expression of TRPV3 mRNA transcripts 48 hours following transfection with either non-coding, scramled RNA (scr-RNA) or siRNA targeting TRPV3 (siRNA). Data are normalized to the average of the untransfected control to indicate the fold change in the TRPV3 expression. Normalized data are presented as mean ± SEM of three independent determination. (G) Effect of siRNA transfection targeting TRPV3 on the Ca^{2+} signals evoked by the indicated agonists. Measurements were carried out at 48 hours after transfection. Averages of the corresponding control treatments on scrambled RNA transfected cells are considered as 100% in each case to control the variance of the effectivity between different agonists and make comparable the effect of the siRNA transfection in the different groups. Data are presented as mean ± SEM, n=6 in each group.